EEET ECOLOGICAL ENGINEERING & ENVIRONMENTAL TECHNOLOGY

Ecological Engineering & Environmental Technology, 2026, 27(9), 70–91
https://doi.org/10.12912/27197050/226004
ISSN 2719–7050, License CC-BY 4.0

Received: 2026.07.03
Accepted: 2026.07.15
Published: 2026.08.15

Energy-saving aeration control for reducing post-harvest losses in semi-arid barley stores using a psychrometric drying-capacity criterion

Charef Eddine Zekri[1*], Amel Yahyaoui[2], Arij Nasfia Hayder[3], Mohamed Amine Hennouni[4], Mohamed Nejib El Melki[1]

[1] Department of Agricultural Engineering, Higher School of Engineers of Medjez El Bab, University of Jendouba, Route du Kef, Km 5, 9070 Medjez El Bab, Béja, Tunisia
[2] Signal, Image and Energy Control Laboratory, Department of Electrical Engineering, National School of Engineers of Carthage, University of Carthage, 45 Rue des Entrepreneurs, Charguia II, 2035 Tunis, Tunisia
[3] Research Laboratory of Thermal and Thermodynamic of Industrial Processes, National Engineering School of Monastir, University of Monastir, 5000 Road Ibn El Jazzar Monastir, Tunisia
[4] Laboratoire des Ressources Naturelles et Aménagement des Milieux Sensibles (RNAMS), Université Larbi Ben M'Hidi W. Oum, El Bouaghi, Tunisia
* Corresponding author's e-mail: charfeddinezekri@gmail.com

ABSTRACT

Aeration control in stored grain was largely developed for temperate climates, where cool air is used to reduce grain temperature. In hot semi-arid stores, however, moisture can be the dominant hazard and the coolest air may also be the most humid. This study evaluated whether aeration should be triggered by the drying capacity of incoming air rather than temperature alone, and assessed the contribution of wall insulation. A psychrometric drying-capacity criterion was tested in two geometrically identical octagonal steel silos containing 3 Mg of barley each; one was bare steel and the other jacketed with 4 cm expanded polystyrene. The silos operated side by side through three regimes in 2025. On a common 768 h autumn block, continuous, fixed-night and temperature-cooling controls were evaluated as counterfactual simulations using the logged weather and grain record and compared with the physically deployed drying-capacity controller. Without ventilation, the insulated silo damped bulk-temperature fluctuations more strongly than the bare silo (53% versus 13%). Simulated continuous ventilation selected air at 72% relative humidity, temperature-cooling control at 75–86%, and fixed-night ventilation at 85%. In contrast, the drying criterion selected air at 39% relative humidity in the bare silo and 44% in the insulated silo. The deployed controller operated for 75 and 40 h, respectively, using air averaging 45% and 36% relative humidity. Fan operation was 61–79% lower than the simulated fixed schedule and 75–95% lower than the simulated temperature-based or continuous strategies. Sensor-inferred grain water activity fell below the indicative mould-growth boundary for more than 92% of hours, and incoming dew point remained below grain temperature except for one marginal hour. Grain sampling every three days detected no insect infestation, although localized moist pockets occurred in the non-insulated silo. From this single instrumented deployment, the results indicate that drying capacity was a more effective aeration trigger than temperature alone under the semi-arid conditions investigated. The low-cost psychrometric controller selected drier air and reduced fan operation while under generally favourable physical storage conditions during this deployment; microbiological safety was not assessed.

Keywords: grain storage, aeration control, psychrometrics, mould growth boundary, low-cost sensing, barley, semi-arid climate.

INTRODUCTION

Much avoidable post-harvest cereal loss begins in the store. There, moulds, mites, and moisture migration spoil grain that arrived sound (Jayas, 2012; Kumar and Kalita, 2017). The store is best read as a managed ecosystem, in which physical, chemical, and biological factors interact

(Jian and Jayas, 2012). The proximate driver of microbial spoilage is the availability of water, measured by the equilibrium relative humidity of the air in the grain pores, or equivalently by grain water activity. Below about 65 to 70% equilibrium relative humidity, storage moulds and mites are suppressed; above it they become active (Magan and Aldred, 2007; Agriculture and Horticulture Development Board, 2023). Temperature acts in two ways. It sets the rate of biological activity, and, where it is spatially uneven, it drives moisture from warm toward cool regions, where condensation can follow (Kenkel and Noyes, 2017).

For malting and food barley, this storage phase is especially sensitive because the technological value of the crop depends not only on preserving mass, but also on preserving physiological and sanitary quality. Small shifts in intergranular humidity can move the bulk from a stable state to a biologically active state, whereas temperature alone does not describe whether water is available to fungi or mites (Agriculture and Horticulture Development Board, 2023). This is why aeration decisions must be read through the coupled temperature-humidity state of the air and the grain, rather than through temperature alone.

Aeration, drawing ambient air through the bulk with a fan, is the standard way to manage the stored-grain environment. The control logic behind many practical systems grew up in temperate agriculture. There the aim is to cool the grain with cool, often nocturnal, air, so the fan is triggered when ambient temperature drops below grain temperature by a useful margin (Kenkel and Noyes, 2017). This logic does not transfer directly to a hot, semi-arid climate. The daytime air is hot but very dry; the night air is cooler but humid; and the binding constraint is keeping the grain dry, not cold. A controller asked to cool will reach for the cool night air, which is also the most humid air on offer. In moisture terms, that is the wrong air to move. Field tests of controllers built for this regime, run against the schedules they are meant to replace, remain rare, even as low-cost open hardware for grain monitoring spreads (Anukiruthika and Jayas, 2025; Liu and Li, 2021). One further question is seldom settled by measurement. Wall insulation is routinely recommended for metal silos, yet its effect on the thermal regime is rarely quantified against an uninsulated control under the same weather.

This climatic inversion creates a practical contradiction for conventional controllers. The hours that are attractive from a cooling perspective are often the hours with the highest relative humidity, whereas the warmer hours may offer the highest drying potential because their absolute moisture load is low. A controller based only on an air-grain temperature difference therefore cannot distinguish between air that cools the grain safely and air that may increase the moisture activity of the intergranular environment. The present work treats this distinction as the central control problem in semi-arid storage.

Gating ventilation on the air's drying capacity rather than its temperature is not, in itself, a new idea. Equilibrium-moisture and dew-point control is long-established practice, and extension guidance recommends ventilating only when the air has drying potential (Kenkel and Noyes, 2017). Simulation-and-data controllers have also adjusted set points to hold safe moisture while saving energy (Lopes et al., 2008), and adaptive aeration schemes have reported large reductions in unit energy use (Gao et al., 2023). The contribution here is therefore not the physical principle alone, but a field demonstration of the principle under semi-arid conditions: a like-for-like comparison of a drying-capacity rule against temperature-based and fixed-time schedules, all scored on the same weather record, plus a check from the actuation log of what the deployed rule actually did. The approach also stands in deliberate contrast to the data-driven, often opaque machine-learning controllers that increasingly dominate this literature (Anukiruthika and Jayas, 2025): because the rule here is three auditable psychrometric inequalities rather than a trained model, an operator can read the reason for every fan decision directly from live sensor values, without retraining for a new site or a new grain once its sorption isotherm is known. Unoptimised aeration also carries a direct energy and food-security cost in semi-arid post-harvest systems, so the present demonstration speaks to the United Nations Sustainable Development Goals on zero hunger (SDG 2) and responsible consumption and production (SDG 12), in addition to the agronomic case made here.

Accordingly, the novelty claimed here is not the underlying psychrometric principle, but its implementation as an auditable low-cost controller and its field demonstration under semi-arid barley-storage conditions.

The research gap is therefore methodological and experimental. Existing guidance establishes the physical principle that aeration should use air with favourable drying potential, but field demonstrations under semi-arid conditions rarely compare, on the same weather record, a drying-capacity controller with the temperature and night-time rules it would replace. This study is not presented as a replicated population trial; it is a mechanistic proof of concept in which first-principle psychrometric inequalities are tested against a full field log. That positioning is important: the transferable claim concerns the control mechanism, whereas the numerical effect sizes require replication.

The objective of this research was to verify, under real semi-arid storage conditions, whether barley aeration should be triggered by the drying capacity of incoming air rather than by ambient temperature alone. The specific objectives were to: (i) formulate a psychrometric rule that can be implemented on low-cost hardware; (ii) compare, on a common 768 h weather block, the air selected by continuous, fixed-night, temperature-cooling and drying-capacity strategies; (iii) verify from the actuation log whether the deployed controller actually followed the drying-capacity mechanism; and (iv) quantify, as a within-deployment case observation, the thermal damping and fan-hour implications of an expanded-polystyrene jacket.

The study was structured around four hypotheses. H1: a psychrometric rule based on dew point, vapour pressure and grain water activity can be expressed as a practical hourly controller without site-fitted constants. H2: the drying-capacity criterion selects substantially drier air than temperature-based or fixed-night operation on the same weather record. H3: automated drying-capacity control reduces fan-hours while keeping the grain mostly below the indicative mould-growth boundary during the automated period. H4: the external expanded-polystyrene jacket damps the bulk temperature swing and therefore lowers the fan-hour demand relative to the bare steel silo in this deployment.

MATERIALS AND METHODS

Experimental design and methodological rationale

The experiment was designed as a field demonstration rather than a replicated agronomic trial. Both silos were exposed to the same external weather and were operated under identical regimes, which allowed the control logic and the insulation effect to be examined without seasonal or site differences between treatments. The uninsulated silo represented the conventional metal structure, whereas the insulated silo represented the same structure protected by an external EPS jacket. Because only one silo was available for each structural condition, differences between the two silos are interpreted as within-deployment evidence and not as population-level estimates.

The experimental design therefore does not provide biological or technical replication in the statistical sense. The two silos were used to obtain a controlled side-by-side field comparison under identical weather forcing, but they cannot support population-level inference about silo type, insulation performance, or controller performance across farms, seasons, grain lots, or storage structures. For this reason, all comparisons between the bare and insulated silos are interpreted as within-deployment observations. The purpose of the study is to test the physical plausibility and operational behaviour of the psychrometric control rule under real semi-arid storage conditions, not to estimate a generalized treatment effect

The methodological sequence followed four steps. First, the physical aeration criterion was defined from dew point, vapour pressure and equilibrium relative humidity. Second, hourly measurements were collected from ambient air and from the grain bulk during the three operating regimes. Third, all competing control strategies were replayed on the same autumn data block so that fan-hours and ventilated-air humidity could be compared under identical weather. Fourth, the realised fan log was analysed to determine whether the automated system actually selected warm, dry air and avoided hours with wetting risk.

Psychrometric aeration criterion

Ventilation should be allowed only when air moving through the bulk removes water, or at least does not add it. Three measurable conditions capture this.

All variables used by the controller were measurable at the hourly time step: ambient temperature, ambient relative humidity, grain temperature and intergranular relative humidity. The criterion was intentionally expressed as inequalities rather than as fitted empirical constants, so that the rule could be transferred to other warm storage contexts once the sorption relationship of the stored grain is known. The three conditions were applied sequentially, meaning that failure of any one condition was sufficient to keep the fan switched off.

No wetting

Incoming air must not deposit water on the grain. This holds when the dew point of the ambient air lies below the grain temperature,

$$Td(amb) < Tgrain \quad (1)$$

where: the dew point was computed with a standard Magnus-type approximation using the coefficients $a = 17.62$ and $b = 243.7$ °C.

These coefficients are those proposed by Alduchov and Eskridge (1996) for an improved Magnus-form approximation over water; recent thermodynamic and observation references are used here only to situate dew-point calculation and the operational use of humidity-derived variables, not to validate those exact coefficients (Romps, 2021; World Meteorological Organization, 2024). Condensation, where warm moist air meets cooler steel and cooler surface grain on the underside of the roof and on the walls, is the recognised moisture-failure mode of metal silos, and it appears once the local relative humidity climbs above about 70% (Molina-Herrera et al., 2025). Condition (1) is the controller's guard against it: air whose dew point exceeds the grain temperature is refused, so ventilation cannot wet the grain.

Net drying

Air removes water from the grain only when its water vapour pressure lies below the vapour pressure in equilibrium with the grain surfaceamb < egrain, e = RH/100 × esat(T),

$$esat(T) = 0.6108\ exp[17.27T/(T + 237.3)]\ \text{kPa} \quad (2)$$

The pore air equilibrates with the grain at its equilibrium relative humidity, so egrain = ERHgrain/100 × esat(Tgrain). The saturation-vapour-pressure term in Equation (2) is a standard Tetens-type expression used here in kilopascals; it is consistent with the equilibrium-moisture framework used for grain storage calculations (American Society of Agricultural and Biological Engineers, 2012). At equal temperature this collapses to the relative-humidity form RHamb < ERHgrain. Ambient and grain are not always at the same temperature, so the relative-humidity comparison is a low-cost proxy rather than the exact rule; in the deployed controller the dew-point condition (1) keeps the incoming air low in absolute moisture, which is what makes the proxy safe in practice. The grain equilibrium relative humidity follows from its moisture content through the barley sorption isotherm (Choi, 2018). Operational ERH ceiling. Ventilation is permitted only while the sensor-inferred grain state remains below the selected moisture-risk boundary,

$$ERHgrain < 75\%,\ water\ activity < 0.75 \quad (3)$$

A 75% ERH operational ceiling was selected as a conservative controller stop threshold in relation to published storage guidance and biological-risk literature. Storage mould activity is commonly associated with equilibrium relative humidity or water-activity conditions beginning in the approximate 65–70% range for susceptible storage ecosystems, while practical cereal-storage guidance links increasing moisture availability with progressively greater deterioration risk (Magan and Aldred, 2007; Agriculture and Horticulture Development Board, 2023). The 75% value was therefore not used as a universal microbiological safety limit or as a site-fitted optimum. Rather, it was adopted as an operational upper boundary that prevents the controller from treating increasingly moisture-active grain as an unrestricted aeration state. The threshold was coupled with the barley sorption relationship of Choi (2018), so its interpretation remained commodity-specific.

The 75% ERH ceiling was therefore used as an operational stop threshold rather than as a claim that fungal growth begins at one universal value or that grain below this threshold is microbiologically safe. A lower threshold would make the controller more conservative and would reduce eligible fan-hours; a higher threshold would increase operating opportunities but would narrow the moisture-risk margin. Consequently, the selected value influences fan duty most strongly during borderline hours. For other cereals, climates or storage objectives, the threshold should be re-evaluated from the relevant sorption isotherm, recommended storage moisture range and biological-risk literature rather than transferred unchanged.

The fan runs only when all three conditions hold. The contrast with a temperate cooling trigger is the crux of the argument. A cooling controller ventilates when

$$Tamb < Tgrain - \Delta T \quad (4)$$

a rule that is silent on humidity. In a semi-arid autumn, the hours that satisfy it are the cool, humid nights, so a cooling controller spends its fan-hours pushing the most humid air available into a bulk whose chief enemy is moisture. The drying criterion does the opposite: it selects the warm, dry daytime air that actually removes water. The fan runs only when all three conditions hold (Figure 1).

Site and the paired-silo demonstration

The demonstration ran at Medjez El-Bab, Béja Governorate, in the Mejerda valley of northern Tunisia, a semi-arid, Mediterranean-influenced cereal region with hot, dry summers. Two geometrically identical octagonal silos (across-flats 1.5 m, 0.2 cm steel wall) each held 3 Mg (3 metric tonnes) of barley, filled to a grain height of 1.70 m above a 0.60 m conical base and below a 0.60 m headspace (Figure 2a). Silo A was bare galvanised steel. Silo B carried a 4 cm external jacket of expanded polystyrene (EPS). The two stood side by side in the open (Figure 2b), so they met the same weather at every instant. The jacketed silo is a within-deployment reference, not a replicated treatment arm: the two share weather, season and grain lot, so the observed divergence is consistent with an insulation effect; however, with one silo per condition, the difference is interpreted as a within-deployment case observation rather than a population-level treatment effect. Each silo had its own 3 kW centrifugal fan.

The paired layout was important for interpretation because ambient temperature, solar radiation, wind exposure and nocturnal humidity changed strongly over the campaign. Placing the two silos side by side made those external forcing variables common to both structures. The comparison therefore focused on the effect of the wall jacket and the control decision, while avoiding the stronger confounding that would arise if the bare and insulated silos were tested during different weather periods.

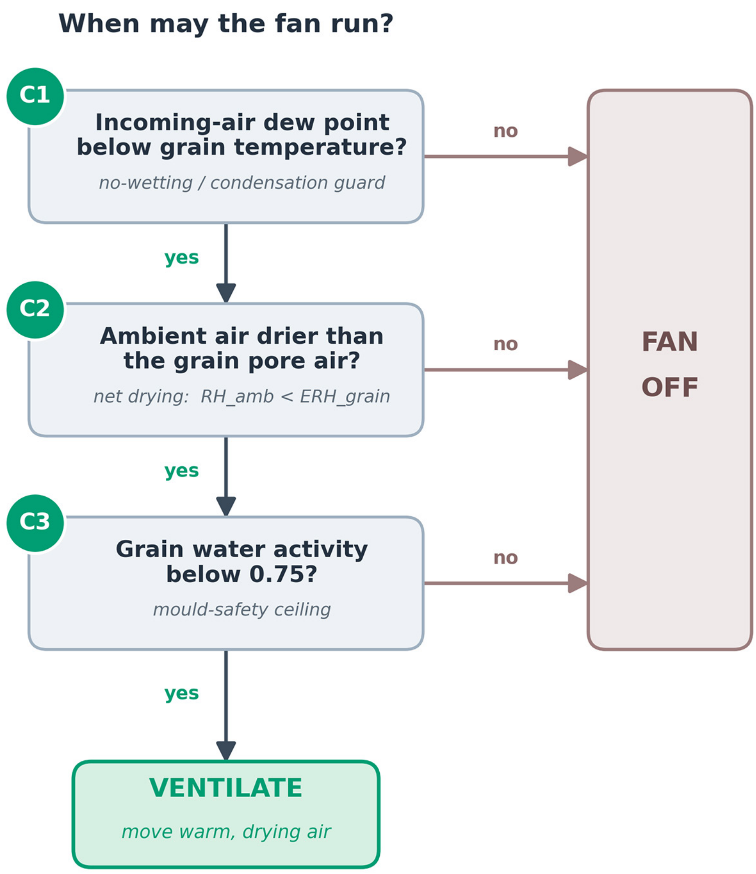

Figure 1. The drying-capacity criterion as a decision rule. The fan runs only when all three conditions hold in sequence: the incoming air's dew point lies below the grain temperature (no wetting), the air is drier than the grain pore air (net drying), and the grain water activity is below the operational ERH ceiling. Any failure leaves the fan off

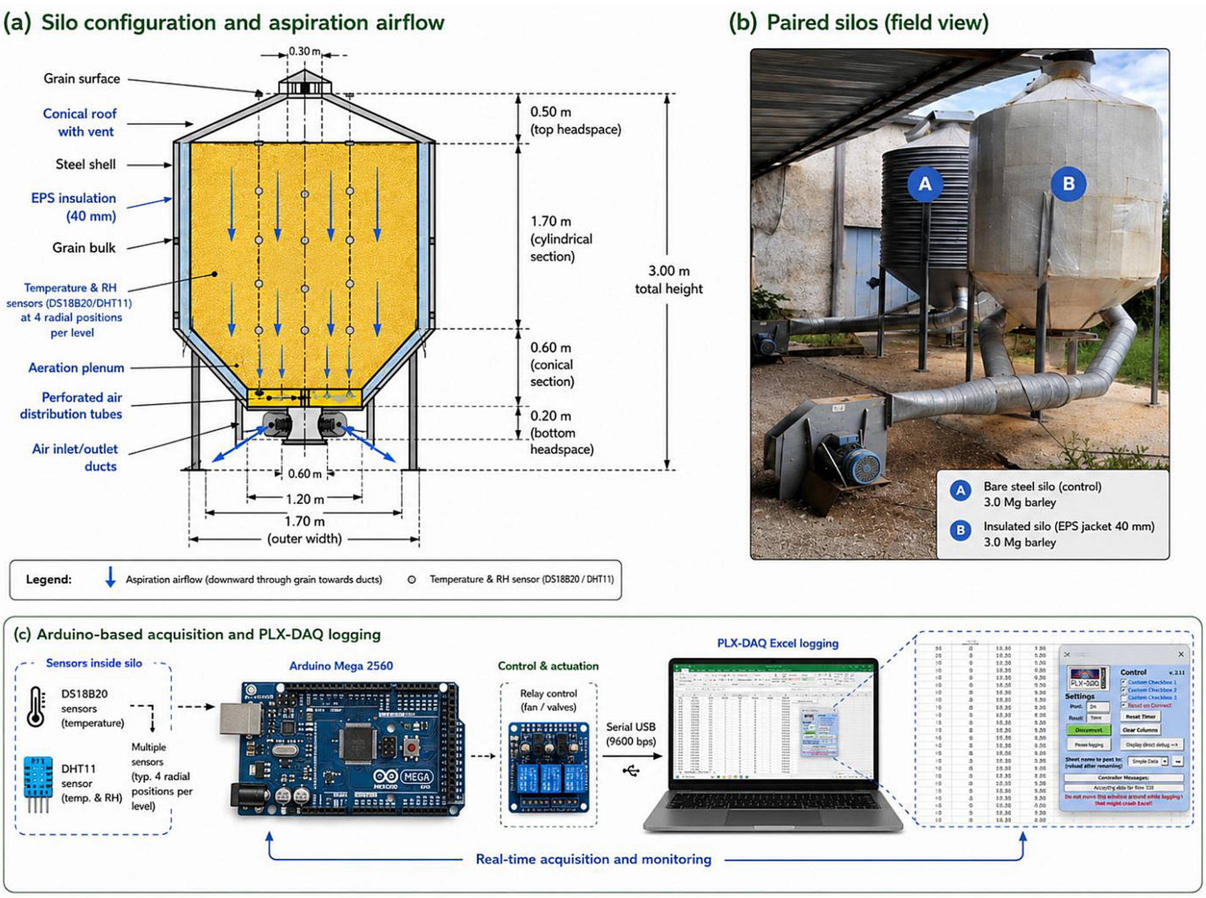

Figure 2. Experimental paired silos used in the study. (a) Cross-sectional view of the silo geometry, showing the 0.60 m top headspace, 1.70 m barley column, 0.60 m conical base, steel wall, EPS insulation jacket, and air ducts, (b) Field view of the two experimental silos: A, bare steel silo; B, EPS-jacketed silo

Instrumentation

Each silo carried DS18B20 digital temperature probes (±0.5 °C) on four layers (heights 17, 62, 107 and 152 cm), reported as layer means, and a DHT11 sensor (±2 °C, ±5% RH) for intergranular-air humidity. A further DHT11 sensor measured ambient temperature and humidity. A single Arduino Mega 2560 logged every channel hourly, with 4.7 kΩ pull-ups on the one-wire lines and relay switching of each fan (Figure 3). The controller and sensing package cost about 180 US dollars, including the Arduino board, temperature probes, humidity sensors, wiring, pull-up resistors, relays and enclosure; it excludes the 3 kW centrifugal fans and the silos themselves.

The DHT11 was selected deliberately as a low-cost, widely available sensor representative of the hardware accessible to small and medium-scale grain stores and compatible with the simple Arduino-based architecture used here. This choice prioritised affordability, replacement availability and straightforward digital integration rather than metrological-grade humidity accuracy. Its ±5% RH tolerance can affect decisions when the measured state lies close to the dew-point, humidity-gap or 75% ERH switching boundaries; accordingly, manufacturer tolerances were propagated through the decision analysis and borderline hours were identified explicitly. For most hours, the observed decision margins were larger than the propagated sensor-error band, whereas 10–17% of hours for the dew-point condition and about 10% for the humidity ceiling were classified as borderline. A higher-accuracy, individually calibrated capacitive humidity sensor would be expected mainly to reduce switching uncertainty and false on/off decisions near these boundaries. It could therefore alter the exact number and timing of fan-hours, but it would not change the three psychrometric inequalities, the physical direction of the control logic, or the finding from this deployment that dry-air selection differed strongly from the retrospectively simulated cooling and fixed-night strategies.

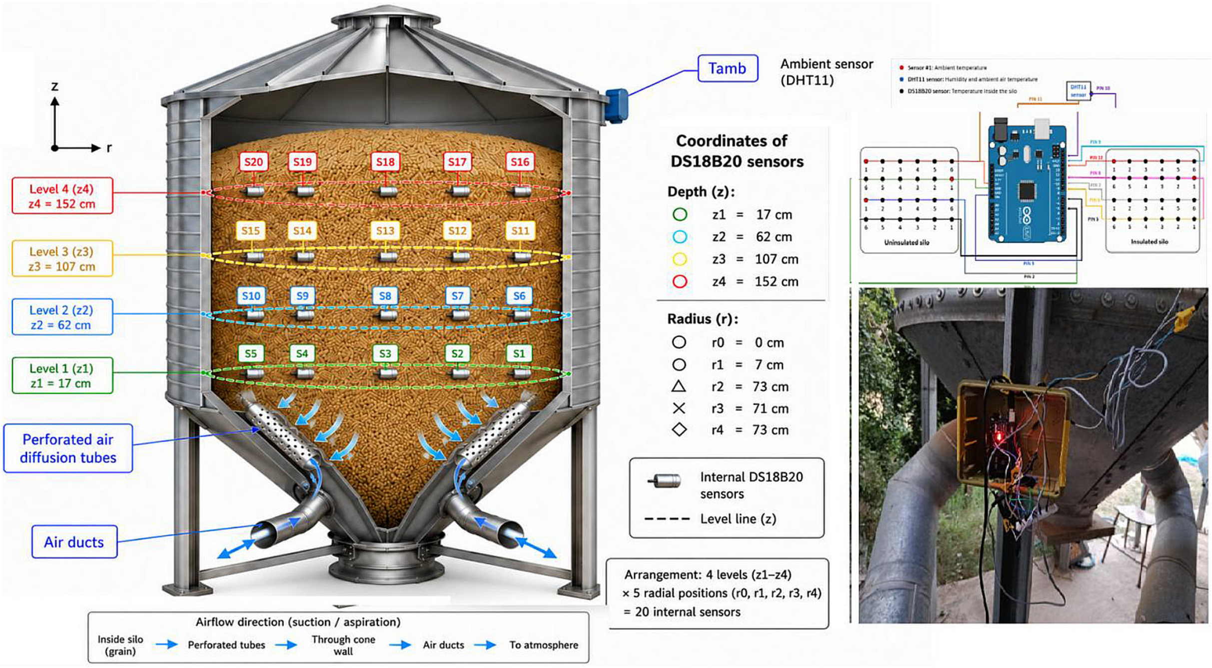

Figure 3. Sensing and control architecture. One Arduino Mega 2560 reads four DS18B20 layers per silo, one ambient DHT11 and one intergranular DHT11 per silo, and switches each fan

The vertical distribution of the DS18B20 probes was chosen to represent the lower, intermediate and upper layers of the grain column. Layer means were used rather than individual probe values because the objective was to characterise the bulk thermal response relevant to aeration decisions.

Before deployment, each series of DS18B20 temperature probes was verified against a calibrated Testo reference probe. The Testo instrument was recalibrated annually by the supplier and served as the traceable reference for verification of the grain-temperature sensors. The DS18B20 probes and the Testo reference probe were exposed simultaneously to the same temperature conditions. The mean absolute deviation between the DS18B20 probes and the calibrated Testo reference probe was 0.19 °C, and the maximum observed deviation was 0.35 °C. Both values were well within the manufacturer-specified accuracy of the DS18B20 probes (±0.5 °C), confirming their suitability for field temperature measurements.

The two DHT11 sensors (ambient and intergranular) were not individually calibrated against a reference hygrometer before deployment. Instead, three complementary validation approaches were used to assess the plausibility and stability of their measurements.

First, the ambient DHT11 was independently compared with hourly records from the Institut National de la Météorologie (INM) synoptic station at Béja (36.73° N, 9.18° E, 158 m a.s.l.), the nearest reference station to the experimental site at Medjez El-Bab (36.63° N, 9.61° E, 69 m a.s.l.; distance ≈ 38 km). The INM station operates meteorological instruments maintained according to World Meteorological Organization recommendations (World Meteorological Organization, 2024). Over the common 768 h autumn block, the ambient DHT11 temperature measurements showed a mean bias of +0.40 °C, a root-mean-square deviation (RMSD) of 0.63 °C and a residual standard deviation of 0.50 °C relative to the INM records. Relative humidity showed a mean bias of −3.18 percentage points, an RMSD of 4.03 percentage points and a residual standard deviation of 2.55 percentage points (Table 4). The correlation coefficients were $r = 0.94$ for temperature and $r = 0.81$ for relative humidity. These results indicate that the DHT11 successfully reproduced the temporal variability of the ambient atmospheric conditions. The magnitude of the observed differences was consistent with the manufacturer-specified tolerances (±2 °C and ±5% RH), although part of the discrepancy may reflect differences in altitude, local exposure and microclimate between the experimental site and the INM station. Therefore, this comparison is interpreted as an independent field validation of measurement plausibility rather than as a traceable laboratory calibration.

Second, the ambient and intergranular DHT11 humidity series were compared as an internal consistency check. Over the 768 h monitoring period, the two humidity series were positively correlated (Pearson r = 0.78), with a physically plausible offset of approximately 8–12 percentage points resulting from grain–air equilibration. No abrupt divergence or progressive drift was detected, indicating stable sensor behaviour throughout the experiment. Because both measurements were obtained using the same sensor model, this comparison was considered an internal consistency assessment rather than an independent accuracy validation.

Third, the temperature measurements were further assessed for physical consistency by comparing the observed grain thermal response with the behaviour expected for bare and insulated steel silos reported in the literature (Lawrence et al., 2013; Molina-Herrera et al., 2025). The measured thermal damping values (12.8% for the bare silo and 53.2% for the insulated silo) were consistent with published results for silos of comparable geometry and insulation thickness, supporting the physical plausibility of the recorded temperature data. This physical-consistency assessment complemented, but did not replace, the direct pre-deployment verification of the DS18B20 probes against the calibrated Testo reference instrument.

Taken together, the pre-deployment verification of the DS18B20 probes against a calibrated reference instrument, the independent comparison of the ambient DHT11 with the INM synoptic station and the internal consistency assessment of the two DHT11 sensors provide complementary evidence that the sensing system operated reliably throughout the deployment. Nevertheless, because the DHT11 sensors were not individually calibrated against a traceable reference hygrometer, the manufacturer tolerances (±2 °C and ±5% RH) were retained and propagated as conservative uncertainty bounds throughout the controller-decision and grain-condition and moisture-risk analyses.

Data were logged hourly because the controller was intended for practical farm use, where the relevant changes in ambient humidity and grain temperature occur over hours rather than minutes. The same logging interval was used for all regimes and for both silos, ensuring that the comparisons of thermal damping, fan-hours and ventilated-air humidity were based on a common temporal resolution.

Regimes and the deployed controller

The silos ran under three regimes in 2025, both always in the same regime at once: no ventilation (28 July to 13 August, 408 h, peak summer); a fixed schedule with fans on from 00:00 to 06:00 daily (14 August to 19 September, 888 h); and automated control under the drying criterion (15 October to 15 November, 768 h, autumn). Each hour, the deployed controller evaluated the three conditions of the psychrometric aeration criterion section and logged its fan state. We treat that log as ground truth.

The three regimes served different purposes in the analysis. The no-ventilation period provided the clearest contrast for thermal damping because no fan operation could modify the temperature response. The fixed-night schedule represented a simple rule commonly used when cool night air is assumed to be beneficial. The automated period tested the proposed criterion under real actuation. Counterfactual strategies were not physically imposed during autumn; instead, they were recomputed from the logged weather and grain series to avoid exposing the grain to potentially humid ventilation.

At each hourly decision, the controller first checked whether the ambient dew point was below the measured grain temperature. It then checked whether the incoming air was drier than the pore-air environment represented by the grain equilibrium relative humidity. Finally, it checked whether the grain remained below the selected operational ERH ceiling. The fan state was set to on only if the three tests were simultaneously true; otherwise, the fan remained off and the reason for rejection was implicit in the failed condition.

Equal-footing comparison of control strategies

The three regimes ran in different seasons, so a direct comparison among them would confound control strategy with weather. To avoid this, we evaluated four strategies on one common block of weather, the 768 h autumn record, using the measured ambient and grain series. Only the drying criterion was physically deployed; the other three strategies continuous running, the fixed schedule and the temperature-cooling trigger are evaluated as counterfactual computations over the measured weather and grain series, so this comparison is a model-free simulation rather than a controlled experiment. For each strategy we counted the fan-hours it would call and, more tellingly, the mean relative humidity of the air it would move through the grain. The four were: continuous running; the fixed 00:00 to 06:00 schedule; a temperature cooling trigger (C); and the drying criterion of the psychrometric aeration criterion section. The deployed controller's logged actuation gives the realised reference. This equal-footing replay was essential because the raw operating regimes occurred in different months. Without this standardisation, a lower fan demand could reflect cooler weather, higher ambient humidity or a different seasonal pattern rather than the control strategy itself. The common-block analysis therefore separated the effect of the decision rule from the effect of weather and allowed the quality of the air selected by each strategy to be compared directly.

Mould growth boundary and other metrics

We characterised the sensor-inferred grain moisture-risk state by placing the measured grain state on the water-activity and temperature plane against an indicative lower boundary for storage-mould growth, set near the xerophilic limit of water activity near 0.70 with mild temperature dependence (Magan and Aldred, 2007). We quantified thermal damping as $1 - \sigma grain/\sigma amb$, the fractional reduction in the standard deviation of the grain-bulk mean temperature relative to ambient. Hourly series are autocorrelated, so we characterised the sampling uncertainty of each damping value with a moving-block bootstrap using 24 h blocks and 4000 resamples. The reported 95% intervals are percentile intervals from the bootstrap distribution. These intervals quantify within-series sampling uncertainty conditional on the single realised weather sequence for each control regime. Because the hourly observations are temporally autocorrelated, the bootstrap confidence intervals describe uncertainty within the observed time series rather than independent experimental replication. Since each structural condition (bare and insulated) and each control regime was observed only once, the bootstrap cannot estimate between-silo, between-season or between-site variability and therefore should not be interpreted as providing population-level confidence intervals. Short gaps in the humidity channels were filled by multivariate imputation with light smoothing and flagged. We assessed sensitivity to the DHT11 by propagating its ±2 °C and ±5% RH tolerances through the dew point and the decision margins.

For each regime, the primary response variables were: the standard deviation of the grain-bulk temperature, the resulting thermal damping relative to ambient air, the number of fan-hours, the mean relative humidity of ventilated air, the fraction of hours below the mould boundary and the dew-point wetting margin. These variables were selected because they correspond directly to the practical objectives of storage aeration: limiting thermal gradients, avoiding wetting, reducing unnecessary fan operation and maintaining favourable grain-storage conditions and limiting moisture-related deterioration risk.

Independent assessment of grain condition

Before silo filling, the barley lot had an initial moisture content of 12.8% on a dry basis (d.b.), equivalent to approximately 11.35% on a wet basis. Immediately after filling, the initial bulk grain temperature in each silo was calculated as the arithmetic mean of the temperatures recorded across all monitored grain layers. This value represented the average thermal state of the complete instrumented grain column rather than the temperature of a single sampling point.

During the experimental period, grain condition was independently monitored every three days. Samples were collected from different depths and locations within the grain bulk using a telescopic grain-sampling probe. The primary purpose of this periodic sampling was to detect insect infestation within the stored grain mass. During each inspection, the samples were also examined for localized moisture accumulation, grain caking, visible fungal development, abnormal odour, discoloration and other signs of deterioration.

These periodic observations were conducted independently of the DHT11 measurements and of the water-activity calculations used in the psychrometric analysis. They therefore provided a direct qualitative assessment of the physical and biological condition of the stored grain throughout the experiment. No microbiological enumeration, fungal identification or mycotoxin analysis was performed.

Data-driven verification

We read the control rule and the moisture-risk margin directly from the logged record. To recover what governs ventilation, we trained three classifiers in scikit-learn: a random forest, a logistic model and a depth-three decision tree (Pedregosa et al., 2011). The hourly fan state was predicted from six physical features: the dew-point depression Tgrain − Td(amb), the grain-to-ambient relative-humidity gap, ambient temperature and humidity, intergranular humidity, and the air-grain temperature difference Tamb − Tgrain. Models were scored by time-blocked cross-validation across five contiguous blocks to reduce temporal leakage between training and testing, and feature influence was read from permutation importance. Because permutation importance can share or distort importance among correlated predictors, its ranking was interpreted cautiously rather than as a causal decomposition (Strobl et al., 2008). For moisture-risk assessment we propagated the DHT11 tolerance by Monte-Carlo: for each hour we drew the intergranular humidity and grain temperature within the sensor band and counted exceedances of the mould boundary, which yields an expected number of hours above the indicative boundary with a credible interval rather than a single count.

The data-driven models were not used to build the controller; they were used only as an independent check of the realised decisions. If the proposed physical argument is correct, variables describing drying capacity, such as dew-point depression and humidity gap, should explain the fan state better than the air-grain temperature difference used by a cooling controller. This verification step therefore tested whether the logged actuation was consistent with the stated mechanism.

RESULTS

Results are presented in the order of the research questions: the within-deployment insulation effect, the common-weather comparison of competing strategies, the realised fan-hours and physical grain-condition indicators under the deployed controller, and the data-driven verification of the physical decision rule. These results test H1 to H4 jointly because the psychrometric rule, the selected air, the actuation log and the insulation response are coupled in the field deployment.

Thermal damping by wall insulation

The criterion, not the jacket, is the main contribution here; but because the silos were matched we can see what insulation did in this deployment, and it is the context for the fan-hour difference reported later. With both silos under the same weather, the EPS jacket cut the temperature swing of the grain bulk much more than bare steel did. Under no ventilation, an ambient standard deviation of 5.66 °C fell to 4.94 °C in the bare silo, a damping of 12.8% with a 95% bootstrap interval of [11.2, 14.1], and to 2.65 °C in the insulated silo, a damping of 53.2% with a 95% interval of [51.7, 55.8]. That is close to a fourfold advantage (Table 1, Figure 4). The same direction held under both ventilation regimes, 38 to 39% for the insulated silo against 7 to 11% for bare steel, although those rows are harder to read cleanly: under automated control the insulated fan ran far less than the bare one, 40 against 75 h, so the ventilated comparison mixes insulation with fan duty. The no-ventilation row is the cleanest contrast. A representative week (Figure 5) shows the insulated bulk tracing a flatter path against the same forcing. The mechanism is the one described in recent silo-thermal modelling: solar loading and the high conductivity of steel heat the wall, whereas the low conductivity of the grain delays redistribution through the bulk; an external 4 cm EPS jacket intercepts part of that load before it reaches the grain (Lawrence et al., 2013; Molina-Herrera et al., 2025). Because the two silos shared the weather at every instant, this within-deployment comparison isolates the insulation effect from weather and seasonal confounding. With one silo per condition we report the magnitude as indicative, context for the fan-hours below rather than a population estimate; a replicated test would be needed to generalise it.

Table 1. Thermal damping by regime and silo, both silos under identical weather. σ in °C; damping = 1 − σ_grain/σ_amb with 95% within-series bootstrap intervals

Regime	σamb (°C)	σbare (°C)	Damping bare	σEPS (°C)	Damping EPS
No ventilation	5.66	4.94	12.8% [11.2, 14.1]	2.65	53.2% [51.7, 55.8]
Fixed schedule	5.60	4.96	11.4% [9.4, 14.7]	3.46	38.1% [35.2, 44.1]
Automated control	5.72	5.31	7.0% [2.6, 10.9]	3.50	38.7% [35.7, 42.6]

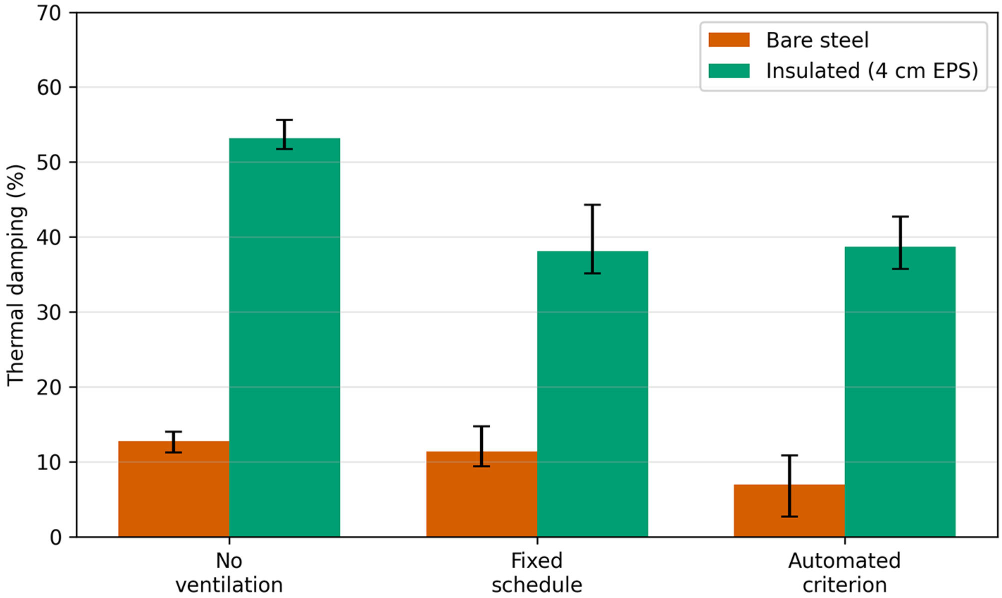

Figure 4. Thermal damping by regime and silo (bars: estimate; whiskers: 95% within-series bootstrap interval). The insulated silo damps the ambient swing three to four times more than bare steel

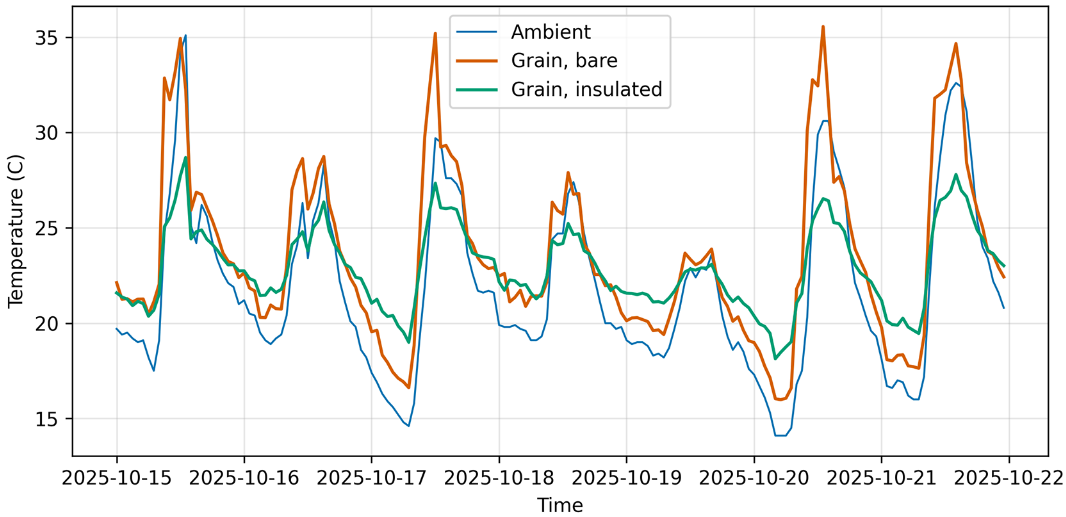

Figure 5. A representative week (automated regime) of ambient air temperature and the layer-mean grain temperature of each silo. The insulated bulk follows a flatter trajectory under the same ambient forcing

Air selected by competing control strategies

The continuous, cooling-trigger and fixed-night strategies discussed below were not run on the silos; they are recomputed as counterfactual simulations on the measured 768 h weather and grain series, for direct comparison with the physically deployed drying criterion reported in the next subsection.The prediction of the psychrometric aeration criterion holds on the field record. Evaluated over the same 768 h of autumn weather (Figure 6), a continuous fan would move air at a mean 72% relative humidity. A temperature cooling trigger would move air at 75%, rising to 86% for the insulated silo, whose cooler grain widens the cool-night window. The fixed night schedule would move the most humid air of all, 85%, because it runs straight through the humid pre-dawn hours. The drying criterion selects air at about 39% relative humidity for the bare silo and 44% for the insulated silo, and it calls the fewest hours. Table 2 focuses on the bare silo to test whether the cooling margin itself explains the result; it does not. The insulated-silo cooling trigger was not repeated in that sensitivity table because the text already reports the more humid 86% case. The lesson is sharp. In a store whose enemy is moisture,

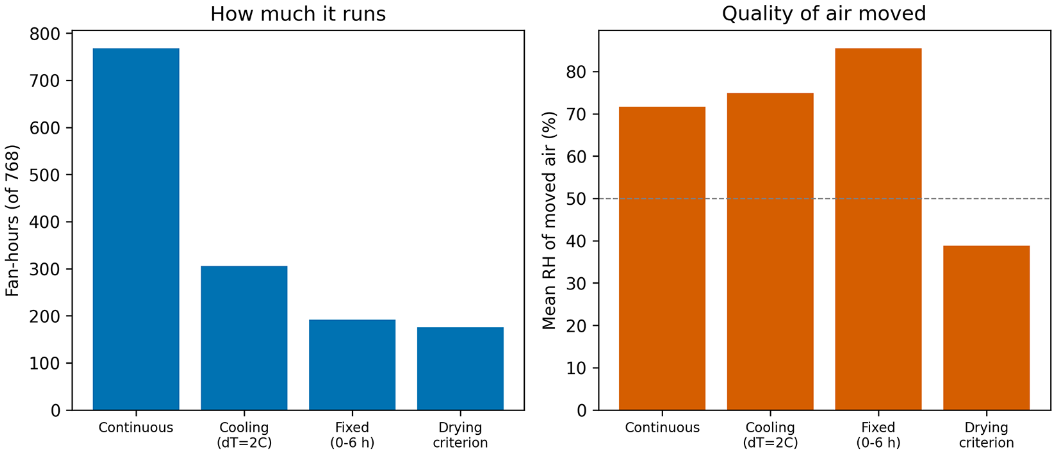

Figure 6. One deployed strategy (drying criterion) and three counterfactual simulated strategies (continuous, cooling, fixed-night) evaluated on the same 768 h of autumn weather (uninsulated silo). The bars represent fan-hours, and the labels represent the mean relative humidity of the air that each strategy would move through the grain. Temperature-based strategies select humid air; the drying criterion selects dry air and runs the fewest hours

Table 2. Simulated cooling-trigger behaviour is insensitive to its temperature margin. Fan-hours and mean ventilated-air relative humidity for Tamb < Tgrain − ΔT, uninsulated silo, common 768 h autumn weather. At every margin it draws humid air; the drying criterion does not

Cooling margin	Fan-hours	Mean ventilated-air RH (%)
ΔT = 1 °C	560	76
ΔT = 2 °C	306	75
ΔT = 3 °C	131	71

temperature-based triggers are not merely less efficient; they ventilate the grain with the wrong air. Changing the cooling margin trades fan-hours but not air quality: at 1, 2 and 3 °C the cooling trigger still draws air at 71 to 76% relative humidity, far above the 39% the drying criterion selects.

Realised fan-hours and ventilated-air quality

The logged actuation matched the criterion's intent. Over the 32-day window the deployed controller ran the bare-silo fan for 75 h and the insulated-silo fan for 40 h, on air averaging 44.8% and 36.3% relative humidity. It left the cool, humid air untouched (74.8% and 73.8% relative humidity during fan-off hours; Table 3). On the psychrometric plane (Figure 7) the fan-on hours form a tight cluster in the warm, dry region. Set against the strategies evaluated on the same weather, this is 61 to 79% fewer fan-hours than the simulated fixed schedule, 75 to 88% fewer than the simulated cooling trigger, and 90 to 95% fewer than simulated continuous running, and the air it moved was about half as humid. The running-time reductions do not depend on fan rating. For the experimental 3 kW fan, they amount to about 0.8 MWh of avoided fan energy across the two silos over the period.

Physical grain-condition indicators during automated control

The sensor-inferred grain state remained below the indicative mould-growth boundary for most, but not all, of the automated period (Figure 8). The bare silo lay below the boundary for 93.8% of hours and the insulated silo for 92.2%, with mean water activity of 0.59 and 0.65. These values describe physical moisture conditions relative to an indicative biological-risk boundary; they do not demonstrate microbiological safety. The 6–8% of hours above the boundary are reported as short sensor-inferred exceedances during the 32-day trial. The incoming dew point stayed below grain temperature in every hour but one, and the fan did not run during that marginal hour, indicating a generally favourable physical wetting margin. Read through the barley sorption isotherm (American Society of Agricultural and Biological Engineers, 2012; Choi, 2018), the mean intergranular humidity was compatible with a relatively dry bulk-average state. Periodic sampling found no insect infestation and no generalized caking, abnormal odour, marked discoloration or extensive visually detectable fungal development, although localized moist pockets occurred in the non-insulated silo. Because fungal

Table 3. Ambient conditions during fan-on and fan-off hours under automated control (mean ± SD). Ventilation was confined to warm, dry air

Variable	Bare fan ON (n = 75)	Bare fan OFF (n = 688)	EPS fan ON (n = 40)	EPS fan OFF (n = 723)
Ambient T (°C)	27.1 ± 5.6	19.6 ± 5.2	28.3 ± 4.8	19.9 ± 5.4
Ambient RH (%)	44.8 ± 20.1	74.8 ± 20.4	36.3 ± 15.3	73.8 ± 20.9
Interpretation	Warm, dry air selected	Cooler, humid air rejected	Warmest, driest air selected	Cooler, humid air rejected

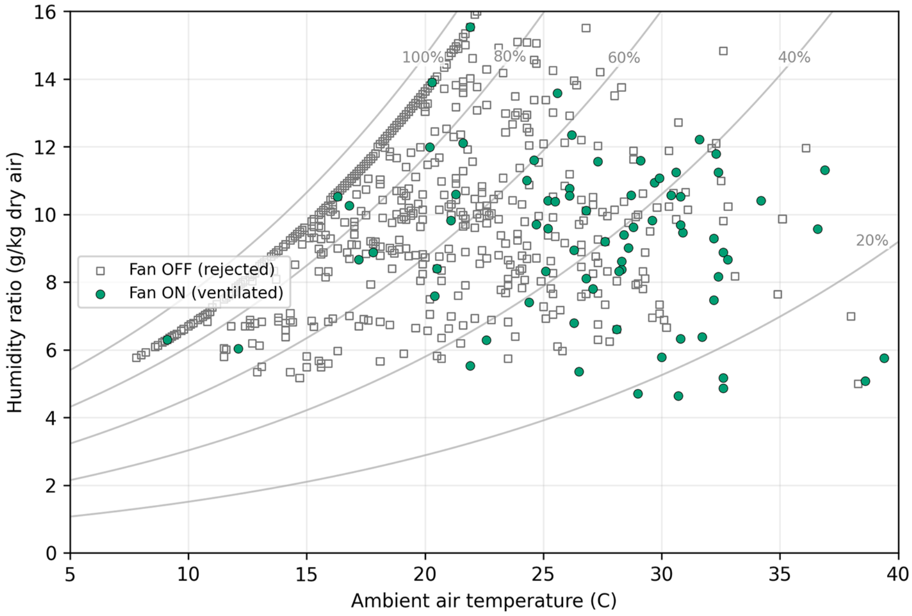

Figure 7. Logged controller decisions on the psychrometric plane (uninsulated silo). Each point is one hour of ambient air; fan-on hours (green) cluster in the warm, low-humidity-ratio region, while the cool, humid hours a cooling controller would chase are rejected. Grey curves are constant-RH lines

populations, microbial counts and mycotoxins were not measured, no conclusion of microbiological safety is drawn.

Independent verification of grain condition

The barley entered storage at an initial moisture content of 12.8% d.b. The initial bulk grain temperature in each silo was calculated as the arithmetic mean of the temperatures measured across all monitored grain layers immediately after filling. Grain samples collected every three days with a telescopic probe showed no evidence of insect infestation in either silo throughout the experimental period. No generalized caking, abnormal odour, marked discoloration or extensive visible fungal development was detected in the sampled grain. A few localized moist pockets were observed in the non-insulated silo, whereas no comparable moisture pockets were detected in the insulated silo. These observations were consistent with the greater temperature variability and lower thermal damping recorded in the non-insulated structure. The moist zones remained localized and were not associated with generalized deterioration or detectable insect infestation during the monitored period. The periodic sampling therefore provided an independent qualitative assessment of grain condition that was consistent with the sensor-based interpretation. Nevertheless, because fungal populations and mycotoxins were not quantified, these observations should not be interpreted as confirmation of microbiological safety.

Robustness to low-cost humidity sensing

The criterion's decisions hold comfortably for most hours once the cheap humidity sensor's error is admitted. The moisture conditions depend on the inexpensive DHT11, so we propagated its tolerances through the decision. The ±5% RH band we carry is a conservative upper bound: independent calibration of the same sensor reports

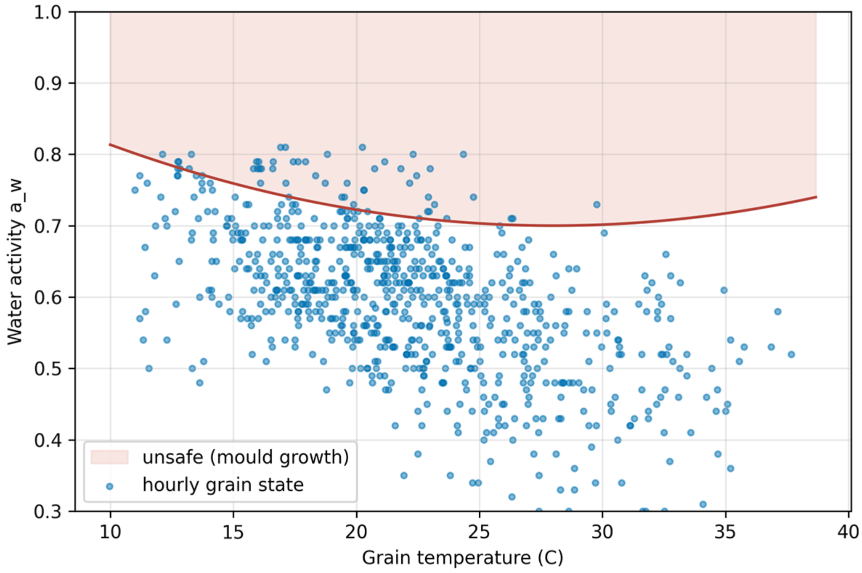

Figure 8. Sensor-inferred grain state under automated control on the water-activity and temperature plane. The solid curve is an indicative lower boundary associated with conditions permitting storage-mould growth; the shaded region above it indicates greater moisture-related biological risk. More than 92% of monitored hours fell below this indicative boundary. The figure describes physical moisture conditions and does not constitute microbiological validation

humidity error well inside it at comparable conditions (Saputri et al., 2025). The ±2 °C and ±5% RH limits translate into a dew-point uncertainty of ±3.2 °C on average, and up to ±7.8 °C in the worst case (Figure 9a). The decision margins were nonetheless comfortable for most hours. The median dew-point margin, grain temperature minus air dew point, was about 6 °C, and the median humidity margin, 75% minus intergranular RH, was 10 to 15 percentage points. Only 10 to 17% of hours for the dew-point condition, and about 10% for the humidity ceiling, fell within the sensor-error band (Figure 9b). The criterion is therefore robust for the majority of hours where margins were large, and the analysis pinpoints the minority of borderline hours in which a calibrated capacitive sensor would harden a production deployment. Propagation bounds the stated tolerance but not unit-specific bias or drift, which were not independently measured in this deployment. The Monte-Carlo propagation therefore quantifies only sensor measurement uncertainty. It is distinct from the within series sampling uncertainty represented by the bootstrap confidence

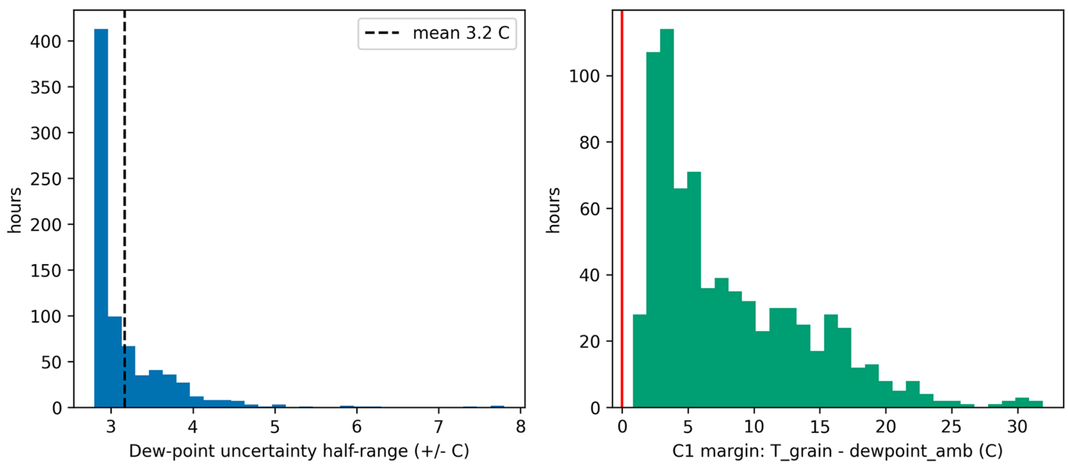

Figure 9. Robustness to low-cost humidity sensing: (a) dew-point uncertainty propagated from the DHT11 tolerances, (b) distribution of the dew-point decision margin; the shaded band marks the minority of hours within the propagated sensor error

intervals and from the between experiment variability that cannot be estimated in the absence of replicated silos or storage campaigns. Published characterisation of these same sensor types under comparable conditions reports accuracy within the manufacturer tolerance propagated here (Saputri et al., 2025; Uddin et al., 2006), so the physical moisture-risk margins are unlikely to be explained solely by the stated sensor tolerance; a gravimetric grain sample would anchor them further and is a priority for a replicated follow-up (the scope and limitations section).

Independent validation of the sensing system

To evaluate the reliability of the sensing system, the ambient DHT11 measurements were compared with hourly observations from the INM synoptic station at Béja during the common 768 h monitoring period. Figure 10 summarizes the comparison.

The two temperature series exhibited nearly identical temporal behaviour throughout the study period (Figure 10a). Linear regression yielded a slope close to unity (1.000), an intercept of +0.41 °C and a coefficient of determination of R^2 = 0.998 (Figure 10c), indicating that the DHT11 accurately reproduced the temporal evolution of ambient temperature. The mean bias was +0.40 °C, the RMSD was 0.63 °C and the residual standard deviation was 0.50 °C (Table 4).

The ambient relative-humidity measurements also closely followed the INM observations (Figure 10b). The regression slope was 0.995 with an intercept of −2.85 percentage points (R^2 = 0.957), indicating a small systematic underestimation of relative humidity (Figure 10d). The mean bias was −3.18 percentage points, with an RMSD of 4.03 percentage points and a residual standard deviation of 2.55 percentage points (Table 4). Comparison of the ambient and intergranular DHT11 sensors showed a strong linear relationship (Figure 10e), consistent with the expected decrease in intergranular humidity caused by moisture equilibration within the grain bulk. The temporal evolution of the residuals (Figure 10f) showed no progressive drift throughout the monitoring period, supporting the stability of the sensing system during field deployment. A detailed analysis of the residual distributions, their dependence on measured values and their hourly behaviour is provided in Supplementary Figure S1.

Data-driven verification of the control rule

The controller follows a deterministic rule, so a classifier trained on its logged hours reproduces the decisions almost exactly (cross-validated ROC-AUC 0.97 for the random forest, 0.94 for logistic). We read that as a consistency check, confirming that the logger and rule behaved as designed, not as a discovery. The informative question is what the decisions depend on once the rule meets real weather. Permutation importance ranks the temperature and dew-point features well above the humidity readings, which add little on their own (Figure 11a). Ventilation probability increased sharply with dew-point depression, whereas it remained comparatively flat against the air–grain temperature difference used by a cooling controller (Figure 11b). The logistic model likewise ranked dew-point depression first; because the temperature features are physically correlated, permutation importance may share credit between them (Strobl et al., 2008). Across the three classifiers, the interpretation was consistent: under the monitored semi-arid weather sequence, the deployed rule responded primarily to drying capacity rather than to cooling potential.

Propagating the humidity-sensor tolerance through the indicative boundary test replaces the hard count with an expected value and a credible interval (Figure 12). The full DHT11 band, carried through a Monte-Carlo analysis, gives an expected 61 h above the indicative mould-growth boundary for the bare silo (95% interval [52, 69]) and 81 h for the insulated silo ([69, 94]) out of 768. Thus, roughly nine hours in ten were estimated to fall below this sensor-inferred boundary, while the expected exceedance count increased relative to the deterministic count once

Table 4. Independent validation metrics for the ambient DHT11 sensor, including mean bias, root-mean-square deviation (RMSD), residual standard deviation, and linear regression statistics relative to the INM Béja synoptic station

Variable	n	Mean bias	RMSD	Residual SD	Slope	Intercept	R^2	Manufacturer tolerance
Temperature	768	+0.40 °C	0.63 °C	0.50 °C	1.000	+0.41 °C	0.998	±2 °C
Relative humidity	768	−3.18 % RH	4.03 % RH	2.55 % RH	0.995	−2.85 % RH	0.957	±5 % RH

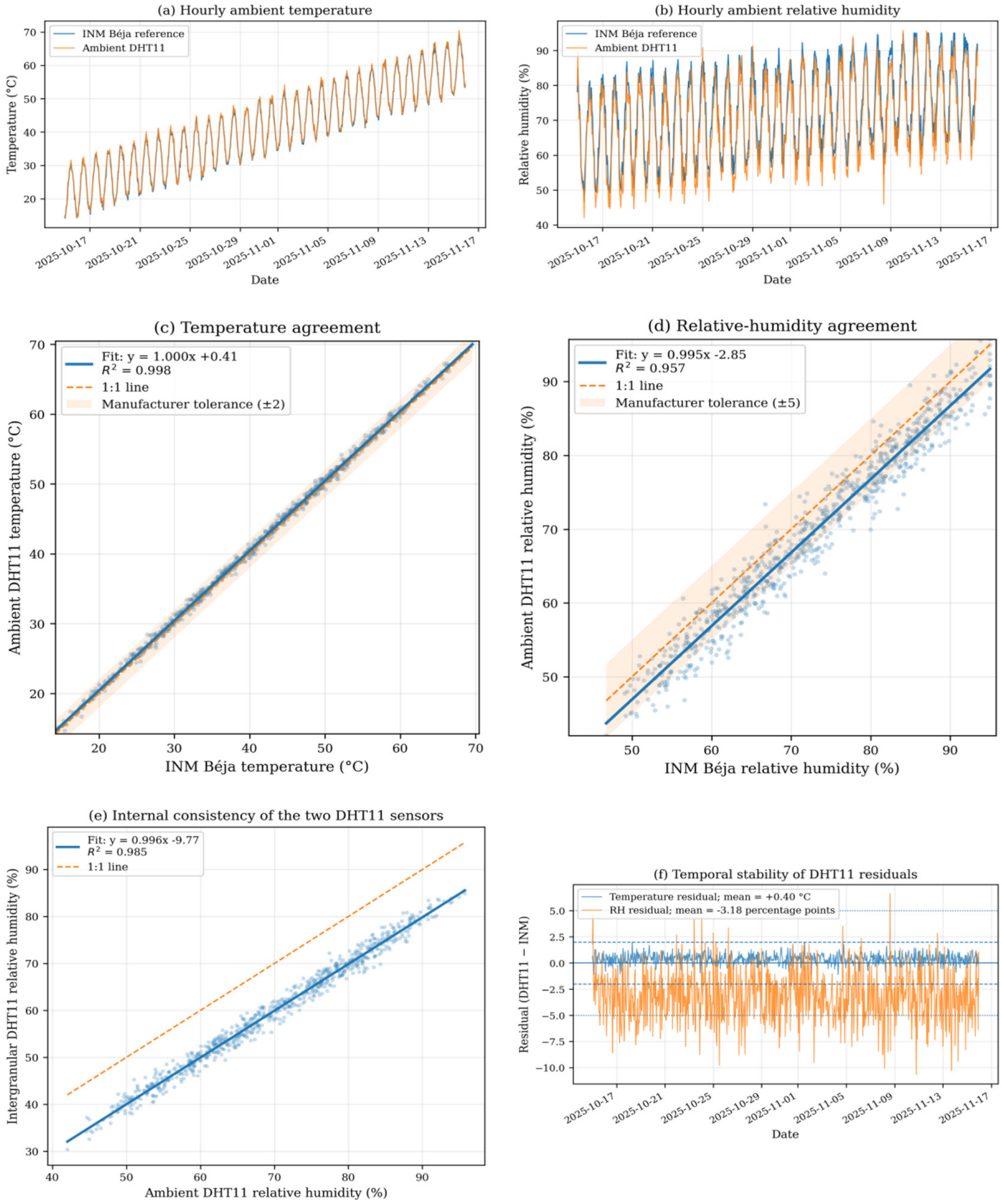

Figure 10. Independent field validation of the ambient DHT11 against the INM Béja synoptic station over the common 768 h autumn block

measurement uncertainty was admitted. These results quantify uncertainty in the physical moisture-state classification only and do not establish microbiological safety. The bare silo, with lower mean sensor-inferred water activity (0.59 versus 0.65), showed fewer hours above the indicative boundary; in this deployment, insulation was associated primarily with thermal steadiness and fewer fan-hours rather than a larger moisture margin. Without microbiological measurements or a gravimetric moisture anchor during the automated period, these remain sensor-based physical-condition estimates.

DISCUSSION

By design this is a single-deployment demonstration: one instrumented store, with a matched second silo as a within-trial reference rather than a replicated treatment arm. The insulation and damping figures are read as case observations rather than population estimates, and the bootstrap intervals describe within-series sampling noise. The absence of replication is the main limitation of the study. Consequently, the results should not be read as proof that the reported fan-hour reductions, thermal damping values, or safety margins

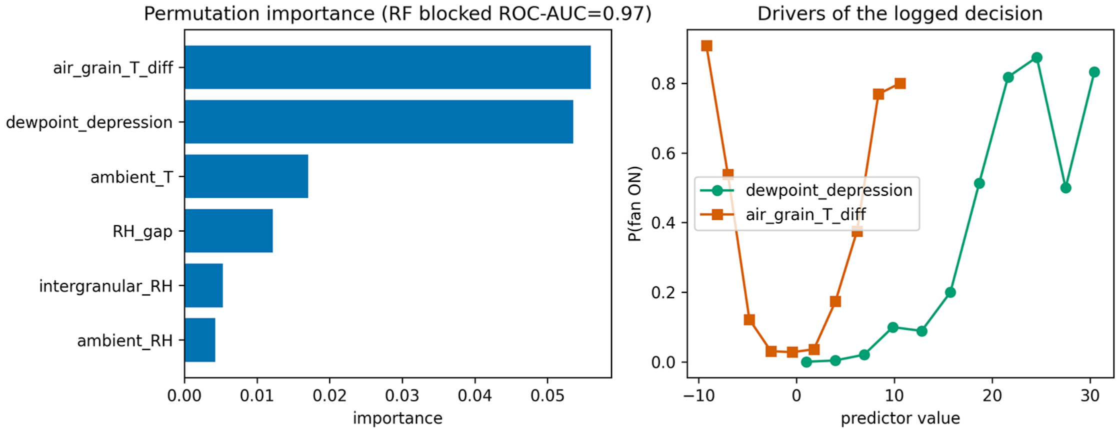

Figure 11. Data-driven recovery of the control rule from the logged hours. (a) Permutation importance for predicting the hourly fan state: the decision rests on the temperature and dew-point structure, not on humidity readings alone. (b) The probability of ventilation rises sharply with the dew-point depression (drying) and is flat against the air-grain temperature difference a cooling controller would use

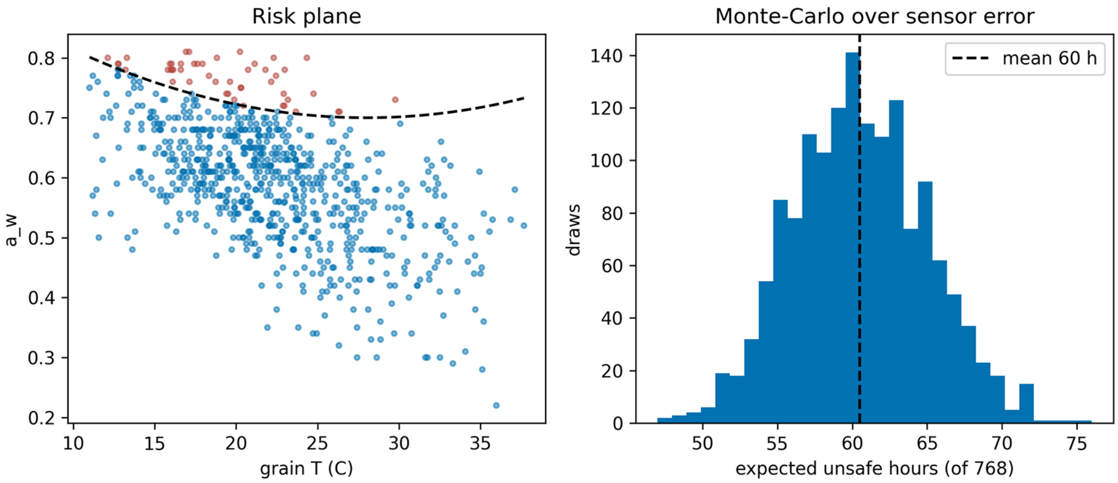

Figure 12. Probabilistic classification of sensor-inferred grain moisture conditions relative to the indicative mould-growth boundary. (a) Water-activity and temperature plane shaded by the propagated probability that the true sensor-inferred state lies above the indicative boundary, with measured hours overlaid. (b) Monte-Carlo distribution of hours above the boundary after propagation of DHT11 tolerance, with the deterministic count marked (dashed). This analysis addresses physical measurement uncertainty and does not validate microbiological safety

would be reproduced quantitatively in other silos or seasons. They should instead be read as evidence that the proposed drying-capacity rule behaved consistently with the expected psychrometric mechanism in this specific field deployment. Replicated trials across additional silos, grain lots, storage seasons, and weather conditions are required before operational recommendations can be generalized. While the mechanism is generalisable, the magnitudes reported here require replication before they can be recommended as standard practice. We do not claim that the 53.2% damping or the 75 and 40 fan-hour counts transfer directly; only the psychrometric inequalities are expected to transfer when the same physical conditions apply.

Statistical limitations

A further limitation concerns the interpretation of the uncertainty intervals reported throughout the study. Three distinct sources of uncertainty should be distinguished. Sensor measurement uncertainty was quantified through Monte-Carlo propagation of the DHT11 measurement tolerance. Within-series sampling uncertainty was quantified using a moving-block bootstrap, which accounts for temporal autocorrelation within the observed hourly record. However, neither procedure estimates the variability expected among independent silos, storage seasons or grain lots. Because one bare silo and one insulated silo were monitored during a single deployment, the present study cannot estimate between-unit variability, and no resampling method applied after the experiment can substitute for true experimental replication. This limitation is inherent to pseudoreplicated experimental designs (Hurlbert, 1984). Consequently, the reported confidence intervals should be interpreted as describing uncertainty within the monitored deployment rather than population-level confidence bounds. The numerical effect sizes are therefore presented as case observations whose generalisation requires confirmation through replicated multi-site experiments

External validation and limits of generalisation. The present work represents one complete field deployment under a single semi-arid weather sequence, one storage season and one barley lot in two small experimental steel silos. The numerical fan-hour reductions, ventilated-air humidity values and thermal-damping magnitudes may not generalise to cold or persistently humid climates, where cooling rather than drying can dominate the aeration objective; to climates with few dry-air windows; to larger or differently shaped stores with different airflow resistance and thermal inertia; to sealed, stirred or mechanically refrigerated systems; to grain batches with higher initial moisture content, different sorption behaviour or heterogeneous fines distribution; or to operating modes with different airflow rates, fan pressures, sensor placement and decision intervals. The EPS response may also change with wall geometry, solar exposure, insulation continuity and air leakage. Although the decision rule is based on general psychrometric relationships rather than site-fitted coefficients, its operational robustness under these conditions remains to be established. Replicated multi-season and multi-site deployments using different grains, storage structures and fan configurations are therefore required before the quantitative performance values observed here are transferred to routine practice.

The independent validation demonstrated that the ambient DHT11 reproduced the temporal evolution of temperature and relative humidity with biases remaining within the manufacturer specifications. Nevertheless, because the DHT11 sensors were not individually calibrated against a traceable reference hygrometer, the INM comparison should be regarded as an independent field validation rather than a metrological calibration.

Similar challenges concerning the balance between affordability, field deployment constraints, calibration requirements, and measurement reliability have been reported for other low-cost environmental monitoring systems based on IoT sensor architectures (Oladosu et al., 2026).

Independent grain-condition monitoring complemented the calculated water-activity assessment. The barley entered storage at 12.8% moisture content on a dry basis, and grain condition was subsequently inspected every three days using samples collected with a telescopic probe. No insect infestation was detected in either silo during the experiment. Only a few localized moist pockets were observed in the non-insulated silo, which was consistent with the larger thermal fluctuations measured in that structure. These direct field observations support the interpretation that the stored grain remained generally stable, while also showing that localized moisture accumulation may occur even when the bulk-average psychrometric indicators remain favourable. However, periodic visual and entomological inspections do not replace microbiological enumeration, fungal identification or mycotoxin analysis. The conclusions have therefore been moderated to refer to favourable physical storage conditions and absence of detected insect infestation, rather than demonstrated microbiological safety.

The results support the central hypothesis of the study: in a semi-arid barley store, the useful trigger for aeration is the drying capacity of the incoming air, not its temperature. The common-weather comparison explains the mechanism. Temperature-based and fixed-night strategies select cool but humid air, whereas the psychrometric criterion selects warm, dry air that has the capacity to remove water from the grain. This distinction is agronomically important because moisture availability, expressed as equilibrium relative humidity or water activity, is the immediate driver of mould risk in stored grain.

The continuous, fixed-night and cooling-trigger alternatives were never independently deployed or experimentally replicated in the silos. Their fan-hours and selected-air characteristics were reconstructed retrospectively by replaying each rule on the same measured 768 h weather and grain record used to evaluate the deployed drying-capacity criterion. Accordingly, the percentage reductions reported against these alternatives are within-dataset counterfactual modeling results, not effect estimates from independent experimental treatment groups.

Within this single deployment the matched silos isolate the jacket's effect cleanly, since both saw the same weather; we read the roughly fourfold damping as a firm case observation rather than a population effect. The two measures compound. By flattening the diurnal thermal load, insulation reduces the work left for the controller, which is why the insulated silo needed barely half the fan-hours of the bare one. The criterion is written in measurable, climate-general quantities rather than fitted constants, so the principle should carry to other warm, semi-arid grains and stores. The size of the insulation benefit, however, will depend on wall geometry, insulation thickness, solar exposure, air leaks, fan design and grain lot. Set against recent field and simulation studies, the present results sit within the same range of reported gains: adaptive moisture-aware aeration of squat silos has been shown to cut unit fan-energy use substantially relative to fixed schedules (Gao et al., 2023), a simulation-and-data controller using set points tuned to hold safe moisture likewise traded a modest rule complexity for energy savings (Lopes et al., 2008), and open low-cost sensing platforms for aeration research have demonstrated that Arduino-class hardware can sustain hourly field logging over months without specialised infrastructure (Liu and Li, 2021). Independent thermal modelling of metal silos under solar loading corroborates the mechanism behind the present insulation result, namely that wall conductivity, not grain conductivity, dominates the diurnal heat input that an EPS jacket intercepts (Molina-Herrera et al., 2025). The present study differs from each of these in scope rather than in direction: the present study differs in scope by combining the physical deployment of a drying-capacity controller with retrospective counterfactual replay of three conventional strategies on the same weather record in a semi-arid climate, and to pair that comparison with a matched insulated and bare silo under identical conditions.

Comparison with recent controllers. Modern humidity-based, equilibrium-moisture and model-assisted aeration systems pursue the same broad objective of avoiding moisture addition while limiting unnecessary fan operation. Simulation-and-data control can tune set points against measured grain and weather states (Lopes et al., 2008), adaptive aeration can modify operation in response to intergranular conditions and energy demand (Gao et al., 2023), and recent AI-oriented grain-storage frameworks increasingly emphasise prediction, multi-sensor integration and data-driven decision support (Anukiruthika and Jayas, 2025). Relative to these approaches, the present controller offers low hardware cost, transparent decisions and direct execution of three auditable psychrometric inequalities without model training, cloud connectivity or site-specific optimisation. These features may be advantageous in low-resource stores and where operators need to understand why the fan was switched on or off. The limitations are equally important: the rule is reactive rather than forecast-based, depends on the quality and placement of low-cost humidity sensors, does not optimise fan speed or electricity tariffs, and does not predict spatial moisture migration within the bulk. More accurate sensing and predictive model-based control could improve decisions near switching boundaries and anticipate future weather windows, but at the cost of additional calibration, computational, data and maintenance requirements. The present study therefore demonstrates a simpler engineering trade-off rather than superiority over modern controllers. Direct replicated field comparisons against contemporary humidity-based and predictive systems remain necessary to quantify relative energy use, grain-condition outcomes and robustness.

More generally, environmental monitoring and control systems increasingly rely on the analysis of meteorological time-series data, where accurate characterization of temporal variability is essential for reliable operational decision-making (Odiana and Yusuf, 2026). Because the three conditions are psychrometric inequalities rather than constants fitted to this site, the logic should carry to other stores where moisture is the hazard and the ambient air is often dry enough to dry the grain: warm, semi-arid and Mediterranean cereal regions, and other grains once their sorption isotherm is known. It does not carry unchanged to cold or persistently humid climates, where cooling is the goal and dry-air hours are scarce, nor to commodities without a known equilibrium-moisture relationship.

Practical implications. The rule is simple to deploy. Run the fan only when three live readings agree: the ambient dew point is below the grain temperature, the ambient relative humidity is below the grain's equilibrium value, and the grain water activity is under 0.75. On this barley store that meant roughly 75 fan-hours over a month rather than the 192 h a fixed night schedule would use. The approximate 180 US dollars refers to the open controller and sensing package only: Arduino board, probes, humidity sensors, relay switching, wiring and enclosure. It does not include the fans, grain silos or insulation materials. This low cost supports practical deployment, but the absence of in-situ calibration means that the humidity channel should be checked against a reference sensor before operational use. For a smallholder, the relevant comparison is not the sensor cost in isolation but the trade-off against the value of the grain it protects and the fan electricity it saves: at roughly 0.8 MWh avoided across the two silos over the 32-day automated period, a single deployment can plausibly recover its hardware cost within one storage season through electricity savings alone, before any reduction in spoilage losses is counted. Two adoption constraints deserve explicit mention. First, the DHT11 sensors and electrical contacts will need periodic cleaning and inspection in a dusty grain-store environment, since dust ingress is a realistic failure mode for low-cost humidity sensing that this short trial could not characterise. Second, the EPS jacket has its own opportunity cost: it adds material and installation expense, occupies space around the silo, and, by this deployment's evidence, mainly buys thermal steadiness and fewer fan-hours rather than additional moisture safety margin, so its value to a given operator depends on local electricity prices and dust or pest pressure on the foam itself. In CO_2 terms, 0.8 MWh of avoided fan electricity corresponds to roughly 0.3 to 0.6 t CO_2 over the trial period using typical North African grid emission factors, a modest but directionally favourable contribution to the energy and emissions footprint of post-harvest storage.

Sensor choice also defines the practical resolution of the controller. In this deployment, the DHT11 was adequate for a low-cost proof of operation because most hourly decision margins were wider than its propagated tolerance and the ambient channel reproduced the temporal variability observed at the INM station. However, the approximately −3.18 percentage-point field bias in ambient relative humidity and the ±5% RH manufacturer tolerance are consequential near the ERH and dew-point switching limits. A higher-accuracy, individually calibrated sensor could shift some borderline hours between fan-on and fan-off states and would be preferable for commercial deployment, especially in humid climates or grain lots operating close to the selected ERH ceiling. The expected benefit is therefore greater decision confidence and potentially different exact fan-hours, not a change in the underlying psychrometric control principle.

CONCLUSIONS

This single field deployment tested whether a psychrometric drying-capacity criterion could control aeration more appropriately than temperature-based logic under the specific semi-arid barley-storage conditions monitored in 2025. In this deployment, the criterion selected markedly drier air and the physically logged controller operated for 75 h in the bare silo and 40 h in the insulated silo. The sensor-inferred grain state fell below the indicative mould-growth boundary for more than 92% of monitored hours, and periodic sampling detected no insect infestation or generalized visually detectable signs of spoilage; localized moist pockets were observed in the non-insulated silo. These observations describe favourable physical storage conditions during the monitored period and do not demonstrate microbiological safety.

In the same deployment, the EPS-jacketed silo showed greater thermal damping than the bare silo under the shared weather sequence, but the observed 53.2% versus 12.8% no-ventilation damping values are case-specific measurements rather than universal insulation effects. Likewise, the reported 61–95% reduction in fan-hours is relative to retrospective counterfactual simulations of continuous, fixed-night and cooling-trigger strategies replayed on the same 768 h dataset; these alternatives were not independently tested in replicated silos. The contribution of the study is therefore the field implementation and mechanistic demonstration of an auditable low-cost psychrometric control rule under semi-arid conditions, not the establishment of universal controller performance coefficients. The exact fan-hours, selected-air humidity and insulation response may change with climate, storage geometry, grain lot, initial moisture content, airflow system, sensor accuracy and operating schedule. Because the experiment used one bare and one insulated silo during one storage season, the quantitative results should be interpreted only as outcomes of this instrumented field deployment. Replicated multi-site and multi-season trials, direct comparison with modern humidity-based and predictive controllers, higher-accuracy calibrated humidity sensing, and microbiological or mycotoxin measurements are required before broader operational or grain-health conclusions can be drawn. Within these limits, the present record supports further evaluation of drying-capacity control as a transparent and low-cost aeration approach for semi-arid grain stores.

Acknowledgements

The authors acknowledge the Higher Institute of Engineers of Medjez El Bab for institutional support and the technical assistance received during the field deployment. Funding: This research received no specific external grant. Data availability and reproducibility: The supplementary package contains the S1–S3 raw hourly datasets, the S4 executable analysis notebook, the S5 reproducibility README, and the S6 Arduino/PLX-DAQ acquisition and control code. The reproducible workflow is: (i) validate the three input filenames, required columns and expected record lengths; (ii) import and harmonise the hourly records and apply the documented quality-control and gap-handling steps; (iii) compute dew point, vapour pressure, equilibrium relative humidity, water activity and hourly controller states; (iv) replay the counterfactual strategies on the common 768 h record; (v) calculate moving-block bootstrap intervals, Monte-Carlo sensor-uncertainty results and time-blocked cross-validation metrics; and (vi) generate the code-derived figures and export the Tables 1–3 analysis summaries. S4 reports the Python, NumPy, pandas, Matplotlib and scikit-learn versions at execution time and writes generated outputs to S4_outputs/. The final package was execution-checked from a clean kernel, and the exact checked environment is recorded in S5. Figure 2 and Figure 3 are non-code visual materials. The independent DHT11-versus-INM validation reported in Table 4 and Figure 10 uses the external paired INM reference series described in the manuscript and is not regenerated from S1–S3; no simulated INM validation data are included or used in the supplementary package.

REFERENCES

1. Agriculture and Horticulture Development Board. (2023). *Grain storage moisture targets for cereals and oilseed rape.* https://ahdb.org.uk/knowledge-library/grain-storage-moisture-targets-for-cereals-and-oilseed-rape
2. Alduchov, O. A., Eskridge, R. E. (1996). Improved Magnus form approximation of saturation vapor pressure. *Journal of Applied Meteorology, 35*(4), 601–609. https://doi.org/10.1175/1520-0450(1996)035<0601:IMFAOS>2.0.CO;2
3. American Society of Agricultural and Biological Engineers. (2012). *ASABE standard D245.5: Moisture relationships of plant-based agricultural products.* ASABE.
4. Anukiruthika, T., Jayas, D. S. (2025). AI-driven grain storage solutions: Exploring current technologies, applications, and future trends. *Journal of Stored Products Research, 111*, 102588. https://doi.org/10.1016/j.jspr.2025.102588
5. Choi, B.-M. (2018). Equilibrium moisture content/equilibrium relative humidity of barley. *Korean Journal of Food Preservation, 25*(5), 543–548. https://doi.org/10.11002/kjfp.2018.25.5.543
6. Gao, G., Wang, X., Wu, J., Li, X., Xu, R., Zhang, X. (2023). An adaptive grain-bulk aeration system for squat silos in winter: Effects on intergranular air properties and grain quality. *Smart Agricultural Technology, 3*, 100121. https://doi.org/10.1016/j.atech.2022.100121
7. Hurlbert, S. H. (1984). Pseudoreplication and the design of ecological field experiments. *Ecological Monographs, 54*(2), 187–211. https://doi.org/10.2307/1942661
8. Jayas, D. S. (2012). Storing grains for food security and sustainability. *Agricultural Research, 1*(1), 21–24. https://doi.org/10.1007/s40003-011-0004-4
9. Jian, F., Jayas, D. S. (2012). The ecosystem approach to grain storage. *Agricultural Research, 1*(2), 148-156. https://doi.org/10.1007/s40003-012-0017-7
10. Kenkel, P., Noyes, R. (2017). *Aeration and cooling of stored grain (Fact Sheet BAE-1101).* Oklahoma State University Extension. https://extension.okstate.edu/fact-sheets/aeration-and-cooling-of-stored-grain
11. Kumar, D., Kalita, P. (2017). Reducing post-harvest losses during storage of grain crops to strengthen food security in developing countries. *Foods, 6*(1), 8. https://doi.org/10.3390/foods6010008
12. Lawrence, J., Maier, D. E., Stroshine, R. L. (2013). Three-dimensional transient heat, mass, momentum, and species transfer in the stored grain ecosystem: Part I. Model development. *Biosystems Engineering, 116*(3), 287-296. https://doi.org/10.1016/j.biosystemseng.2013.08.004
13. Liu, J., Li, P. (2021). Control and real-time data

acquisition of an experimental platform for stored grain aeration study. *Sensors, 21*(16), 5403. https://doi.org/10.3390/s21165403

14. Lopes, D. C., Martins, J. H., Lacerda Filho, A. F., Melo, E. C., Monteiro, P. M. B., Queiroz, D. M. (2008). Aeration strategy for controlling grain storage based on simulation and on real data acquisition. *Computers and Electronics in Agriculture, 63*(2), 140–146. https://doi.org/10.1016/j.compag.2008.01.014
15. Magan, N., Aldred, D. (2007). Post-harvest control strategies: Minimizing mycotoxins in the food chain. *International Journal of Food Microbiology, 119*(1–2), 131–139. https://doi.org/10.1016/j.ijfoodmicro.2007.07.034
16. Molina-Herrera, F. I., Quemada-Villagómez, L. I., Calderón-Ramírez, M., Martínez-González, G. M., Jiménez-Islas, H. (2025). Three-dimensional modeling of natural convection during postharvest storage of corn and wheat in metal silos in the Bajío region of Mexico. *Eng, 6*(9), 224. https://doi.org/10.3390/eng6090224
17. Odiana, S., Yusuf, D. D. (2026). Time series modelling and forecasting of temperature and rainfall in Nigeria using ARIMA models. *Trends in Ecological and Indoor Environmental Engineering, 4*(3), 17–27. https://doi.org/10.62622/TEIEE.026.4.3.17-27
18. Oladosu, M. A., Abah, M. A., Odimgbe, E. I., Adewale, F. E., Arthur, C., Ajayi, A. S., Ezeani, J., Ede, F. O., Oladosu, O. A., Ohanele, E. C. (2026). Smart electrochemical sensors and IoT for monitoring heavy metals in Nigerian water: Review of advances and deployment challenges. *Trends in Ecological and Indoor Environmental Engineering, 4*(1), 79–89. https://doi.org/10.62622/TEIEE.026.4.1.79-89
19. Pedregosa, F., Varoquaux, G., Gramfort, A., Michel, V., Thirion, B., Grisel, O., Blondel, M., Prettenhofer, P., Weiss, R., Dubourg, V., Vanderplas, J., Passos, A., Cournapeau, D., Brucher, M., Perrot, M., Duchesnay, E. (2011). Scikit-learn: Machine learning in Python. *Journal of Machine Learning Research, 12*, 2825–2830.
20. Romps, D. M. (2021). Accurate expressions for the dew point and frost point derived from the Rankine-Kirchhoff approximations. *Journal of the Atmospheric Sciences, 78*(7), 2113–2136. https://doi.org/10.1175/JAS-D-20-0301.1
21. Saputri, F. R., Linelson, R., Salehuddin, M., Nor, D. M., Ahmad, M. I. (2025). Correction: Design and development of an irrigation monitoring and control system based on Blynk Internet of Things and ThingSpeak. *PLOS ONE, 20*(6), e0326137. https://doi.org/10.1371/journal.pone.0326137
22. Strobl, C., Boulesteix, A.-L., Kneib, T., Augustin, T., Zeileis, A. (2008). Conditional variable importance for random forests. *BMC Bioinformatics, 9*, 307. https://doi.org/10.1186/1471-2105-9-307
23. Uddin, M. S., Armstrong, P. R., Zhang, N. (2006). Accuracy of grain moisture content prediction using temperature and relative humidity sensors. *Applied Engineering in Agriculture, 22*(2), 267–273. https://doi.org/10.13031/2013.20273
24. World Meteorological Organization. (2024). *Guide to instruments and methods of observation (WMO-No. 8).* World Meteorological Organization. https://community.wmo.int/site/knowledge-hub/programmes-and-initiatives/instruments-and-methods-observation-programme-imop/guide-instruments-and-methods-observation-wmo-no-8-0
25. Yulizar, D., Soekirno, S., Ananda, N., Prabowo, M. A., Perdana, I. F. P., Aofany, D. (2023). Performance analysis comparison of DHT11, DHT22 and DS18B20 as temperature measurement. In *Proceedings of the 2nd International Conference on Science Education and Sciences 2022 (ICSES 2022)* (pp. 37–45). Atlantis Press. https://doi.org/10.2991/978-94-6463-232-3_5